Effect of VEGF–targeted antisense gene therapy on retinoblastoma cell line SO–RB50 *in vitro* and *in vivo*

Guo-Hong Xin [1], Xin-Han Zhao [1], Dong Liu [2], Qiang Gong [3], Lei Hou [1], Jing-Yun Li [3], Bo-Rong Pan [4], Xu Li [5], Ya-Jie Cheng [1]

[1]Department of Medical Oncology, the First Affiliated Hospital, School of Medicine, Xi'an Jiaotong University, Xi'an 710061, Shaanxi Province, China

[2]Central Hospital of Jiading District, Shanghai 201800, China

[3]The Third Hospital of Baoding, Baoding 071000, Hebei Province, China

[4]Oncology Outpatient Department, Oncology Institute, the Fourth Military Medical University, Xi'an 710032, Shaanxi Province, China

[5]Shaanxi Tumor Hospital, Xi'an 710061, Shaanxi Province, China

Correspondence to: Xin-Han Zhao. Department of Medical Oncology, the First Affiliated Hospital, School of Medicine, Xi'an Jiaotong University, Xi'an 710061, Shaanxi Province, China. zhaoxinhan@mail.xjtu.edu.cn

Abstract

• AIM: To evaluate the possibility of generation 4 polyamidoamine (G4PAMAM) dendrimers acting as the delivery system of vascular endothelial growth factor (VEGF) antisense oligodeoxynucleotides (VEGFASODN), and to investigate the anti-tumor effect of G4PAMAM/VEGFASODN complex on the cultured cells and the mouse tumor xenograft model.

• METHODS: The transfection efficiency was assessed by Flow cytometry (FCM). Thiazolyl tetrazolium (MTT) assay was performed to determine the relative growth rate (RGR) of the cells after transfection. Then a mouse tumor xenograft model of human retinoblastoma was established. Different interventions were given to the mice by intratumoral injection and the tumor growth was monitored. The expression of VEGF mRNA was detected by reverse transcription PCR (RT-PCR), the expression of VEGF protein was determined by western blot analysis, and the microvessel density (MVD) was measured by immunohistochemistry (IHC) staining.

• RESULTS: G4PAMAM/VEGFASODN exhibited a high transfection rate *in vitro*, and the transfection rates of different doses of G4PAMAM/VEGFASODN groups increased with higher doses. This effect was accompanied by a dose-depended reduction in cell viability. The tumor growth in the tumor-bearing athymic mice was significantly inhibited in the G4PAMAM/VEGFASODN group. The expressions of VEGF mRNA and protein were obviously inhibited in the G4PAMAM/VEGFASODN group ($P<0.05$), and the MVD of the G4PAMAM/VEGFASODN group was lower than that of the other groups($P<0.05$).

• CONCLUSION: VEGFASODN can be delivered into the cultured and transplanted retinoblastoma cells efficiently by G4PAMAM, suppress the expressions of VEGF mRNA and protein, and reduce the MVD of tumor tissues. The G4PAMAM/VEGFASODN complex has antitumor properties *in vitro* and *in vivo*.

• KEYWORDS: vascular endothelial growth factor; antisense oligonucleotides; generation 4 polyamidoamine; angiogenesis; gene therapy; retinoblastoma

INTRODUCTION

Retinoblastoma is the most common primary intraocular malignancy in childhood. Although many treatment modalities including plaque radiotherapy, external beam radiotherapy (EBR), laser photocoagulation, cryotherapy, thermotherapy, chemotherapy and enucleation are currently available [1], finding a safer and more efficient treatment modality remains a major challenge [2,3].

Angiogenesis is the essential process of new blood vessel formation to support the tumor growth, development and metastasis [4–7]. In 1971, Dr. Folkman proposed the hypothesis that preventing or destroying the blood supply of a tumour would block its development. It is now generally accepted that angiogenesis is a rate-limiting process in tumor growth [8]. Without new blood vessels formation to provide nutrients and to remove catabolic products, tumor cells

cannot sustain proliferation and thus are likely to remain dormant [9, 10] and tumors cannot grow beyond $2mm^3$-$3mm^3$ [11]. The understanding of the vital role of angiogenesis in cancer growth and metastasis has led to immense interest in research regarding its regulatory mechanisms and clinical implications in the management of cancer patients in the past three decades. Angiogenesis is a multi-factorial and tightly controlled biological or pathological process regulated by many pro- and anti-angiogenic factors and many angiogenic regulators have been identified [12]. In homeostatic conditions, there is very limited new blood vessel growth in the majority of tissues due to the delicate balance between angiogenic activators and inhibitors secreted either by tumor cells or by cells of the tumor microenvironment. However, angiogenesis is initiated when there is a predominance of pro-angiogenic factors [13, 14] and the point at which angiogenesis is triggered is termed as angiogenic switch. So anti-angiogenic therapy may be a promising strategy for cancer treatment due to the vital role of angiogenesis in the process of occurrence, progression, invasion and metastasis of malignant tumors.

VEGF is a primary promoter of both physiological and pathological angiogenesis [15,16], which binds to VEGFR and neuropilin (Nrp) and transmits proliferative signals to downstream molecules. VEGF can stimulate proliferation and migration and prevent apoptosis of endothelial cells, regulate vascular permeability [17], enhance chemotaxis and homing of bone marrow derived vascular precursor cells (both endothelial cells and pericytes) [18,19]. In addition to having pro-angiogenic effects, VEGF also has direct effects on tumor cell survival, migration and invasion, and can also suppress immune function [20]. Therefore, anti-VEGF strategy is an attracting avenue of anti-angiogenic therapy. In fact, anti-VEGF therapy has already showed anti-tumor effects [21-23]. Monoclonal antibodies targeted VEGF or VEGFR, VEGF traps (genetically engineered VEGF-binding proteins) and VEGF receptor protein-tyrosine kinase inhibitors are three commonly used strategies to block VEGF function, but they have only extracellular effects. Downregulation of VEGF through gene therapy can take anti-VEGF effects both intracellularly and extracellularly.

Antisense oligodeoxynucleotides (ASODN) are synthetic single-stranded oligonucleotides designed to target the complementary sequence in the target mRNA. Once delivered into the cell, they hybridize to the mRNA by Watson – Crick base pairing to specifically interfere with gene expression and inhibit protein production. Although the naked ASODN have demonstrated clinical efficacy particularly in combination with conventional anticancer agents [24], improvement of tumor-directed delivery and cellular uptake remains crucial to completely translate the concept of antisense gene therapy into clinical application.

Vectors play critical roles in gene therapy and the loading capacity and transfection efficiency are the most crucial characteristics of vectors. Viral vectors and non-viral vectors are two mainly categories of gene delivery systems in current use. As gene transferring vectors, though retro virus possesses the characteristic of high transfection efficiency, it can carry limited quantity of genes because of its small size. Liposome can carry a larger amount of genes, but the liposome gene delivery system is unstable and has poor tissue specificity and relative low transfection efficiency. Polyamidoamine (PAMAM) dendrimers (one type of nanoparticles) belong to non-viral vectors and can be divided into G0 (generation 0), G1, G2, until G11 PAMAM according to the number of terminal amino groups [25]. They are highly branched spherical macromolecules, nonimmunogenic, and can mediate the delivery of single-stranded and double-stranded, natural or synthetic DNA or RNA [26]. The mechanisms by which dendrimers efficiently transfer genes have been extensively explored [27, 28]. PAMAM dendrimers protect DNA by sterically blocking the access of nucleolytic enzymes [29], which prolong the survival time of DNA in the body. In contrast to the complexes of other generations of PAMAM dendrimers and DNA, G4PAMAM/DNA complex has advantages such as small and uniform particle size, high stability, high transfection efficiency and low toxicity [28-31].

MATERIALS AND METHODS

Preparation of transfection complex G4PAMAM colloid (Starburst™; Sigma Company) was dissolved in sterile triple-distilled water in mass concentration of 10g/L. Seventy seven milligrams VEGFASODN (5'-TGGCTTGAAGATG TACTCGAT-3', phosphorothioate-modified; synthesized by Beijing Aoke Inc.) was dissolved in sterile triple-distilled water in mass concentration of 10g/L. The above two solutions were incubated at room temperature for 10 minutes and then mixed together at charge ratio of 1:40 (VEGFASODN to G4PAMAM). The mixture was incubated at room temperature for 20 minutes and stored at 4℃. Seventy seven micrograms VEGFASODN and 0.5mL Lipofectamine (Invitrigen Company) were combined and incubated for 15 minutes at room temperature and stored at 4℃.

Detection of transfection efficiency *in vitro* SO-RB50 (Shanghai Institute of Chinese Academy of Sciences) cell suspension (3×10^7/L, 500µL) was seeded into a 24-well plate and incubated at 37℃ overnight till the cells went into the exponential growth phase. Eight groups, *i.e.* control group, G4PAMAM group, Lipofectamine/VEGFASODN group and five groups received different doses of G4PAMAM/VEGFASODN (1, 3, 10, 30 and 100µg in VEGFASODN, respectively), were set up, with five wells in each group for duplication validation. Serum-free RPMI

1640 medium was replaced with standard medium 4 hours later. Then the cells were digested with 2.5g/L trypsin after incubation for 24 hours. After digestion was ended, the cell suspension was centrifuged and the supernatant was aspirated. After transfecting with fluorescein isothiocyanate (FITC)-labelled VEGFASODN, the cellular uptake of VEGFASODN was determined by flow cytometry (FCM). The transfection experiment was carried out for three times.

MTT assay SO-RB50 cell suspension (5×10^7/L, 200μL) was added to a 96-well plate and incubated at 37℃ overnight till the cells went into the exponential growth phase. Eight groups, *i.e.* control group, G4PAMAM group, Lipofectamine/VEGFASODN group and five groups received different doses of G4PAMAM/VEGFASODN (1, 3, 10, 30 and 100μg in VEGFASODN, respectively), were set up, with five wells in each group for duplication validation. Serum-free RPMI 1640 medium was replaced with standard medium 4 hours later and the cells were collected for MTT assay after incubation for 24 hours, respectively. MTT (5g/L, 20μL; Sigma Company) was added to each well. The plate was incubated for another 4 hours and the supernatant was aspirated. The cells were washed twice, added with 150μL DMSO (Sigma Company) and vibrated. Finally the absorbance values were read at 490nm with the multi-functional microplate test system and the RGR was calculated according to the following formula: Relative growth rate (RGR) (%) $= A_E / A_C \times 100\%$, where A_E is the absorbance in experimental group and A_C is the absorbance in control group.

Establishment of nude mice model of transplanted retinoblastoma The animal research protocol was approved by Animal Care and Use Committee of Xi'an Jiaotong University. Each Balb/cnu-nu athymic mouse (Shanghai Silaike Laboratory Animal Co. Ltd) was injected subcutaneously in the right flank with 0.2mL cell suspension containing a total of about 5×10^6 SO-RB50 cells. The tumor formation rate was 83.3% (25 of 30) two weeks after inoculation. The tumor growth status was monitored every other day. The tumor size was monitored and recorded and the tumor volume was calculated according to the following formula: volume = (length of short axis)^2×(length of long axis) ×0.5. In the fifth week after inoculation, when subcutaneous nodules grew up to about 100mm^3, one of the tumor-bearing mice was randomly dismissed and the remaining tumor-bearing mice were randomly divided into 4 groups, 6 mice per group and normal saline, G4PAMAM, VEGFASODN (10mg/kg), and G4PAMAM/VEGFASODN (10mg/kg in VEGFASODN), 200μL each, were given by intratumoral injection every other day for ten injections, the tumor size was monitored and recorded for 4 weeks after intervention and then animals were killed. Fresh tumor tissue were dissected, placed in formalin and stored at -70℃ .

Detection of VEGF protein by Western blot VEGF protein was detected by Western blot analysis with standard protocol. Tumor tissues (100mg per mouse) were shredded and placed on ice for 40 minutes in 0.5mL of ice-cold cell lysis buffer. Shredded tissues were homogenized and centrifuged at 14 000g for 10 minutes at 4℃ . The total protein concentration in tissue homogenates was determined with the BIO-RAD protein assay kit (BIO-RAD, USA) with bovine serum albumin used as control. Proteins were separated by 100g/L sodium dodecylsulfate-polyacrylamide gel electrophoresis (SDS-PAGE) and transferred to polyvinylidene difluoride (PVDF) membranes. The membranes were preincubated with skimmed dry milk, probed for VEGF and β$_2$-MG and finally visualized by enhanced chemiluminescence. The VEGF expression was normalized against β$_2$-MG expression and determined by densitometry with three experiments.

RT−PCR analysis The total RNA was extracted with the Trizol RNA extraction kit (Invitrigen Company). cDNA was synthesized with reverse transcription kit (MBI Company) according to the manufacturer's guidelines. cDNA was amplified with specific primers for VEGF (sense, 5'-AGGC GAGGCAGCTTGAGTTA-3'; antisense, 5'-AGGAAGA GG AGACTCTGCGC-3'), and β$_2$-MG was used as internal control. PCR was carried out under the following conditions: denaturized at 94℃ for 30 seconds, annealed at 55℃ for 30 seconds, and extended at 72℃ for 60 seconds. The PCR products were separated in 20g/L agarose gel stained with ethidium bromide (0.5g/L), and photographed. The band intensities were quantified by Quantity One Analysis System. Results were shown by grey degree ratios of VEGF to β$_2$-MG.

Determination of MVD by IHC staining Paraffin imbedded sections were dewaxed, hydrated, blocked, incubated with 50μL rat antihuman CD34 monoclonal antibody (Beijing Zhongshan Jinqiao Co. Ltd) at 37℃ for one hour and washed, and then incubated with 40μL-50μL biotin-labeled goat anti-rat IgG (Beijing Zhongshan Jinqiao Co. Ltd) at 37℃ for one hour and washed. DAB was added to develop color and the response was observed by microscope. The nuclei were counterstained mildly by hematoxylin. Finally the sections were dehydrated by ethanol, exposed to xylene and mounted by neutral resin. Microvessels were counted with a light microscope. The areas containing the greatest number of microvessels, namely 'hot spots', were identified at low magnification (40×) and the microvessels in the hot spots were counted at 100 × magnification. A single, countable microvessel was defined as any vessel with lumen and endothelial cells or endothelial cell cluster brown-stained. The MVD of each tissue was measured in three distinct fields per hot spot. The MVD was expressed as the mean±SD for each group, under
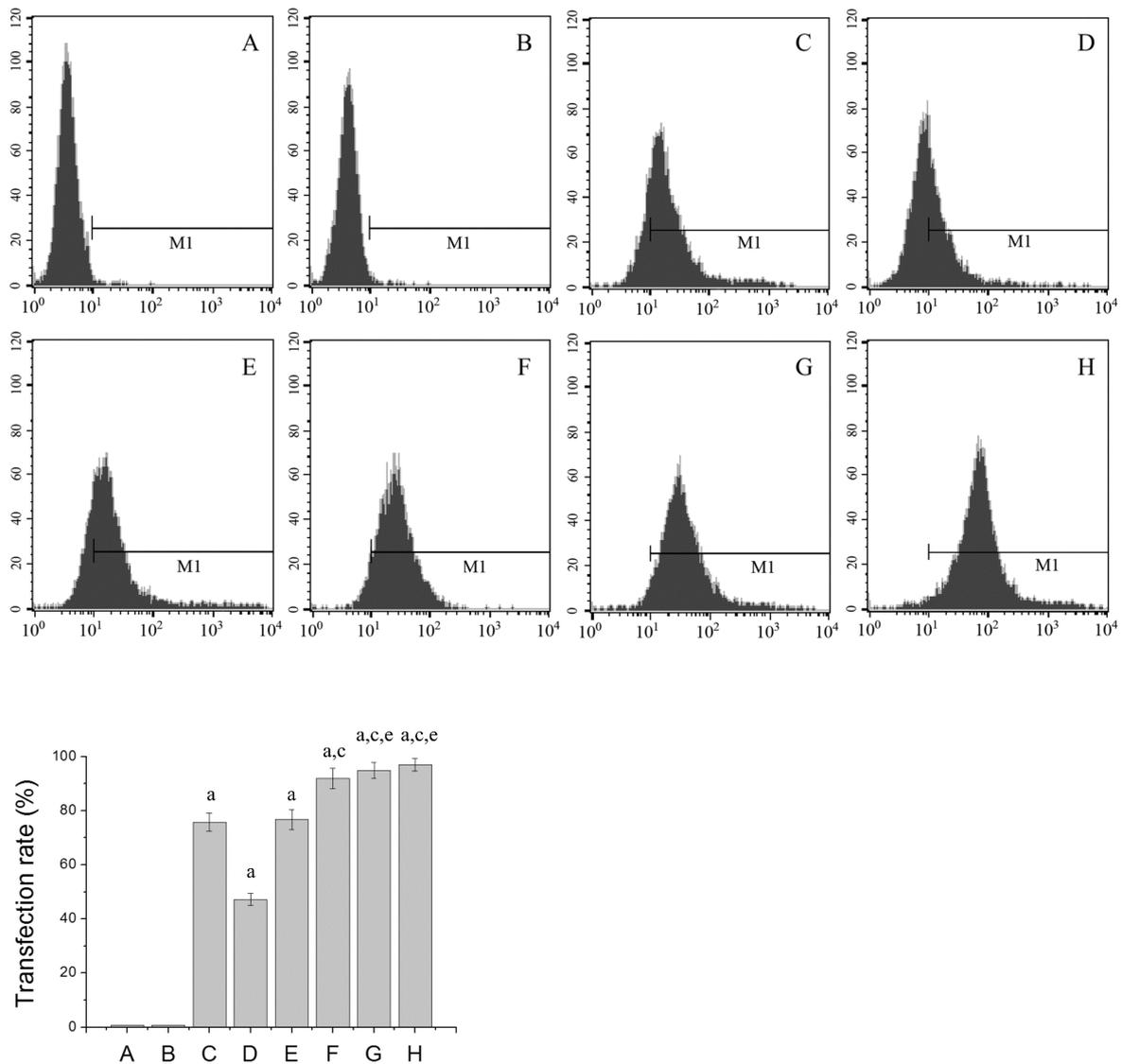
Figure 1 Transfection rates of different groups. G4PAMAM/VEGFASODN exhibited a high transfection rate *in vitro*, and the transfection rates of different doses of G4PAMAM/VEGFASODN groups increased with higher doses A: Control group; B: G4PAMAM group; C: Lipofectamine/VEGFASODN group; D: G4PAMAM/VEGFASODN group (1μg in VEGFASODN); E: G4PAMAM/VEGFASODN group (3μg in VEGFASODN); F: G4PAMAM/VEGFASODN group (10μg in VEGFASODN); G: G4PAMAM/VEGFASODN group (30μg in VEGFASODN); H: G4PAMAM/VEGFASODN group (100μg in VEGFASODN). [a] $P < 0.05$ *vs* control; [c] $P<0.05$ *vs* Lipofectamine/VEGFASODN; [e] $P> 0.05$ *vs* G4PAMAM/VEGFASODN (10μg in VEGFASODN).

the observations of two readers.

Statistical Analysis All of the data was processed with SPSS 16.0 statistical analysis software and expressed in mean ± standard deviation (SD) manner. Single-factor analysis of variance was used to compare among the groups and the test level was $\alpha=0.05$.

RESULTS

G4PAMAM/VEGFASODN exhibited a high transfection rate *in vitro* The transfection rates of each group were detected by FCM 24 hours after transfection with FITC-labelled VEGFASODN. It was found that the transfection rates of different doses of G4PAMAM/VEGFASODN groups and the Lipofectamine/VEGFASODN group were higher than those of the other groups (47.31± 2.16%, 76.69±3.61%, 92.01±3.76%, 94.87±2.93%, 96.92±

2.32% and 75.76±3.44% *vs* 0.79±0.08% and 0.71±0.05%, $P<$ 0.05), the transfection rates of several G4PAMAM/ VEGFASODN groups (10μg, 30μg and 100μg in VEGFASODN) were higher than that of the Lipofectamine/VEGFASODN group (92.01±3.76%, 94.87± 2.93% and 96.92±2.32% *vs* 75.76±3.44%, $P<0.05$), and the transfection rates of different doses of G4PAMAM/ VEGFASODN groups increased with higher doses (Figure 1).

Cell viability suppressed by G4PAMAM/VEGFASODN The cell viability was determined by MTT assay. The results showed that the RGR of cells in different doses of G4PAMAM/VEGFASODN groups and the Lipofectamine/ VEGFASODN group were lower than those of the other groups (72.40±6.94%, 42.72±4.46%, 24.39±2.07%, 21.15± 2.01% and 19.23±1.99% *vs* 98.60±1.30% and 100.00%, $P<$

0.05). The RGR of cells in several G4PAMAM/VEGFASODN groups (10, 30 and 100μg in VEGFASODN) were lower than that of the Lipofectamine/VEGFASODN group (24.39± 2.07%, 21.15±2.01% and 19.23±1.99% vs48.69±3.12%, P< 0.05), and the suppression on cell viability caused by G4PAMAM/VEGFASODN was dose-dependent (Figure 2).

Inhibition of tumor growth in nude mice model The nude mouse model of transplanted retinoblastoma was established and the tumor-bearing mice were photographed immediately after sacrificed (Figure 3). The nude mice were observed every 2 other days and the tumor growth curves of nude mice were drawn (Figure 4). It was found that the tumor growth in G4PAMAM/VEGFASODN group and VEGFASODN group were markedly retarded than those in other groups (P<0.05), and G4PAMAM/VEGFASODN had a stronger inhibitory effect than VEGFASODN (P<0.05).

VEGF mRNA expression suppressed by G4PAMAM/ VEGFASODN The results of reverse transcriptive PCR showed that there were specific 541bp VEGF mRNA bands and 408bp β_2-MG bands in each group, which verified the quality of the template and the accuracy and specificity of primers (Figure 5). It could be seen that the VEGF mRNA of the G4PAMAM/VEGFASODN group and the VEGFASODN group were lower than those of the normal saline group and the G4PAMAM group (0.3619±0.0347 and 0.5962±0.0477 vs0.8310±0.0750 and 0.8298±0.0736, P< 0.05). The VEGF mRNA of the G4PAMAM/VEGFASODN group was lower than that of the VEGFASODN group (0.3619±0.0347 vs0.5962±0.0477, P<0.05).

VEGF protein expression down regulated by G4PAMAM/VEGFASODN The protein expression levels of VEGF and the endogenous control, β_2-MG, were detected by Western blot (Figure 6). The results showed that the expression of VEGF protein of the G4PAMAM/VEGFASODN group and the VEGFASODN group were lower than that of the normal saline group and the G4PAMAM group (0.3671± 0.0352 and 0.5923±0.0488 vs0.9070±0.0756 and 0.8763± 0.0728,P<0.05), and VEGF protein of the G4PAMAM/ VEGFASODN group was lower than that of the VEGFASODN group (0.3671±0.0352 vs0.5923±0.0488, P<0.05).

MVD decreased by G4PAMAM/VEGFASODN The microvessel in tumor tissue was marked with CD34 by IHC staining and counted with a light microscope (Figure 7). The MVD of the G4PAMAM/VEGFASODN group and the VEGFASODN group were lower than those of the normal saline group and the G4PAMAM group (6.5860±0.5766 and 10.5000±0.8163 vs15.4320±1.2039 and 14.9760±1.0668, P< 0.05), and the MVD of the G4PAMAM/VEGFASODN group was lower than that of the VEGFASODN group (6.5860±0.5766 vs10.5000±0.8163, P<0.05).
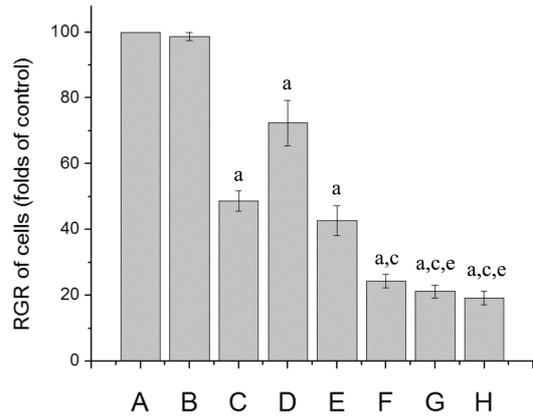
Figure 2 Cell viability of different groups. G4PAMAM/ VEGFASODN decreased the RGR of cells and the suppression on cell viability was dose −dependent A: Control group; B: G4PAMAM group; C: Lipofectamine/VEGFASODN group; D: G4PAMAM/VEGFASODN group (1μg in VEGFASODN); E: G4PAMAM/VEGFASODN group (3μg in VEGFASODN); F: G4PAMAM/VEGFASODN group (10μg in VEGFASODN); G: G4PAMAM/VEGFASODN group (30μg in VEGFASODN); H: G4PAMAM/VEGFASODN group (100μg in VEGFASODN). [a]P< 0.05 vscontrol; [c]P<0.05 vsLipofectamine/VEGFASODN; [e]P>0.05 vsG4PAMAM/VEGFASODN (10μg in VEGFASODN).
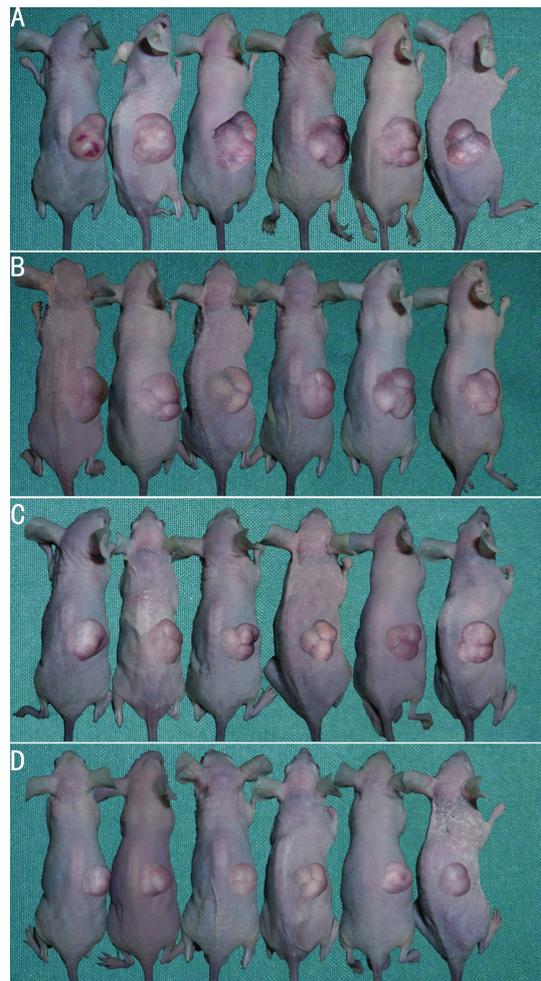

Figure 3 Xenograft tumors of different groups (The pictures were taken immediately after the mice were sacrificed) A: Normal saline group; B, G4PAMAM group; C: VEGFASODN group; D: G4PAMAM/VEGFASODN group.
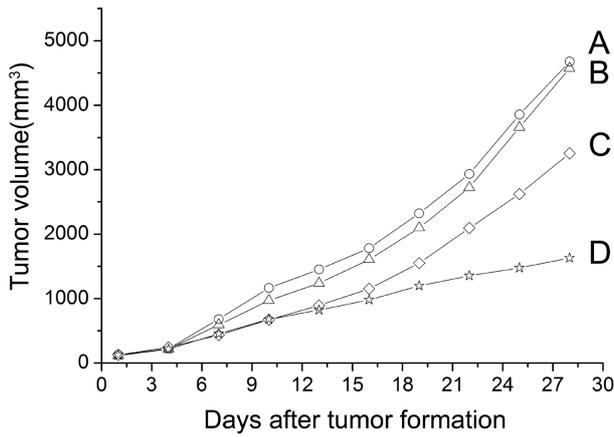
Figure 4 Tumor growth curves of different groups. The tumor growth in G4PAMAM/VEGFASODN group and VEGFASODN group were markedly retarded than those in other groups ($P<0.05$), and G4PAMAM/VEGFASODN had a stronger inhibitory effect than VEGFASODN ($P<0.05$) A: Normal saline group; B: G4PAMAM group; C: VEGFASODN group; D: G4PAMAM/VEGFASODN group.

Figure 6 Expression of VEGF protein. G4PAMAM/VEGFASODN inhibited the expression of VEGF protein A: Normal saline group; B: G4PAMAM group; C: VEGFASODN group; D:G4PAMAM/VEGFASODN group. [a] $P<0.05$ *vs* normal saline; [c] $P<0.05$ *vs* VEGFASODN.
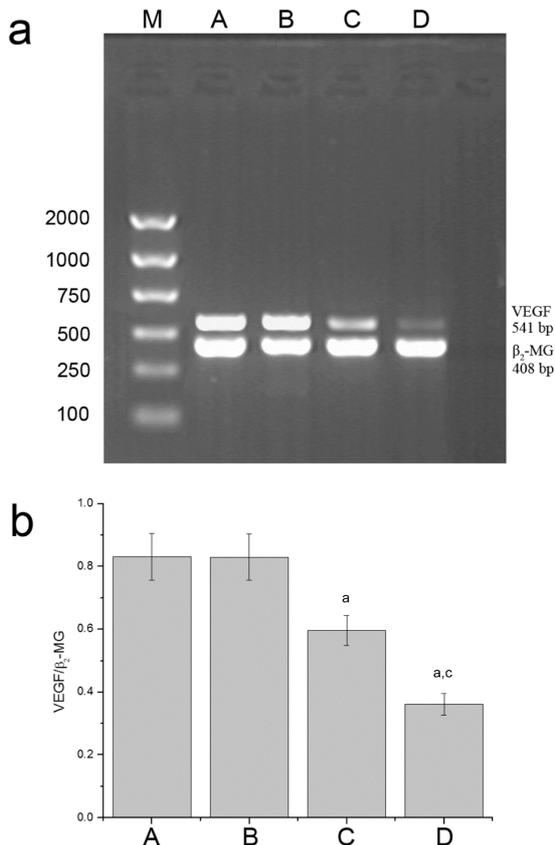

Figure 5 Expression of VEGF mRNA. G4PAMAM/VEGFASODN suppressed the expression of VEGF mRNA M: Marker; A: Normal saline group; B: G4PAMAM group; C: VEGFASODN group; D: G4PAMAM/VEGFASODN group. [a] $P<0.05$ *vs* normal saline; [c] $P<0.05$ *vs* VEGFASODN.

Figure 7 MVD of different groups. G4PAMAM/VEGFASODN decreased the level of MVD A: Normal saline group; B: G4PAMAM group; C: VEGFASODN group; D: G4PAMAM/VEGFASODN group. [a] $P<0.05$ *vs* normal saline; [c] $P<0.05$ *vs* VEGFASODN.

DISCUSSION

In this study, we synthesized G4PAMAM/VEGFASODN and evaluated its transfection efficiency *in vitro* It was found that VEGFASODN was successfully transfected into
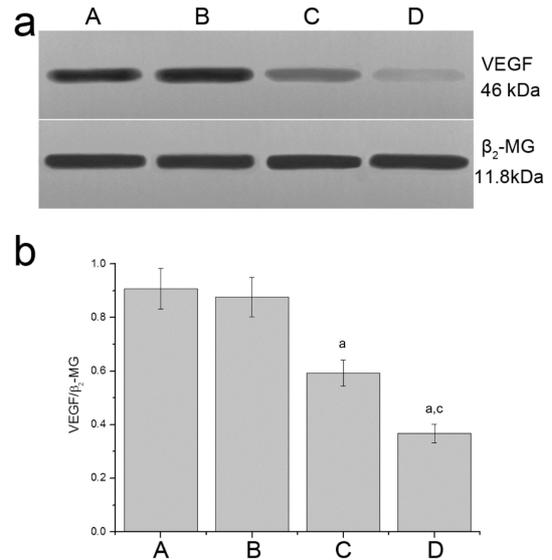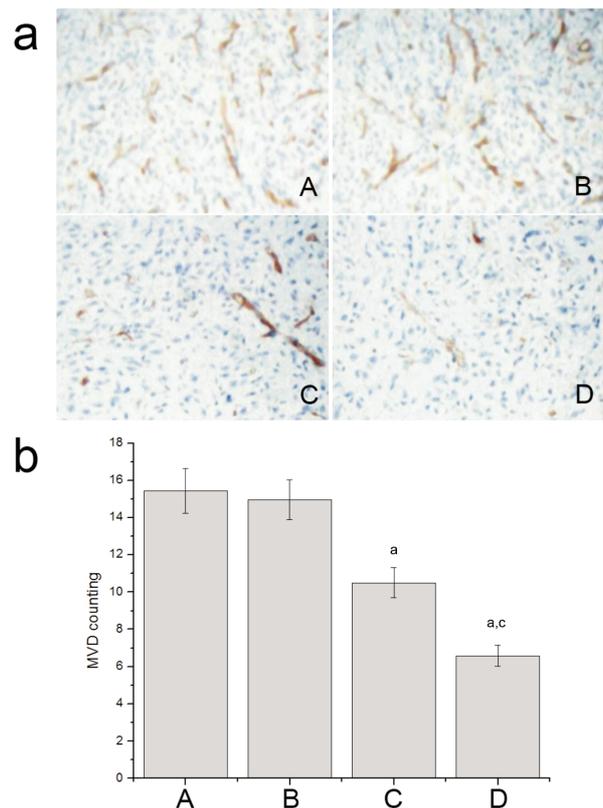
SO-RB50 cells mediated by G4PAMAM dendrimers and the transfection rates of different doses of G4PAMAM/VEGFASODN groups increased with higher doses. The enhanced transfection rate of nucleic acids through PAMAM

can be ascribed to high ability to condense nucleic acids (due to high densities of periphery amines of the PAMAM molecule) and multiple internalization routes [32]. And then it was confirmed that G4PAMAM/VEGFASODN inhibited the growth of cultured human retinoblastoma SO-RB50 cells with MTT assay. G4PAMAM/ VEGFASODN had the best inhibitory effect and the inhibitory effect was dose-depended. The *in vitro* experiments showed that VEGFASODN was delivered into cultured cells efficiently by G4PAMAM and inhibited cell viability. These results are in line with our previous study in which an inhibitory effect on cultured breast cancer cells was observed after G4PAMAM/ VEGFASODN was administered [33].

To further study the *in vivo* effects of G4PAMAM/ VEGFASODN on tumor, mouse tumor xenograft model of human retinoblastoma cell line SO-RB50 was established, then different interventions were administered by intratumoral injection and the tumor growth in mice was monitored, finally the expression of VEGF mRNA and VEGF protein, and MVD in the tumor tissue of each group were detected. The results demonstrated that the tumor growth of G4PAMAM/VEGFASODN group was slower than those of the other groups. Although the tumor growth of VEGFASODN group was slower than those of the normal saline group and G4PAMAM group, it was faster than that of the G4PAMAM/VEGFASODN group. The VEGF mRNA and protein and MVD levels of G4PAMAM/ VEGFASODN group were significantly lower than those of VEGFASODN group, G4PAMAM group and normal saline group. These results are in consistent with those of the previous study that, after administration of chemically synthesized VEGF siRNA, a decrease of VEGF expression, MVD and tumor growth was observed [34]. These effects could be explained that, when introduced into the tumor cells in the body, G4PAMAM/VEGFASODN could targetedly inhibit the expression of VEGF in the tumor cells, thereby reduce the angiogenesis and subsequently slow the growth of the tumor.

In summary, our study showed that G4PAMAM/ VEGFASODN suppressed the proliferation of retino-blastoma (SO-RB50) cells, reduced VEGF mRNA and VEGF protein expression, inhibited tumor angiogenesis, and consequently restrained tumor growth in retinoblastoma bearing mice. A new strategy of gene therapy targeting VEGF has been proposed.

However, it is known that tumor development is a multi-factor regulated and multi-step process. Though inhibition of VEGF alone can decrease angiogenesis and retard tumor growth, the combining inhibition of VEGF and other pro-angiogenic or pro-proliferative molecules has been confirmed to have much more better antitumor effect. Further studies should be focused on the blockade of multi-target or multi-signaling pathway to acquire enhanced antitumor effect in the future.

REFERENCES

1 Balmer A, Zografos L, Munier F. Diagnosis and current management of retinoblastoma. *Oncogene* 2006;25(38):5341−5349

2 Long H, Zhou B, Jiang FG. Expression of MMP−2 and MMP−9 in retinoblastoma and their significance. *Int J Ophthalmol* 2011;4(5):489−491

3 Shan GY, Zhang JH, Lü YG, Yun J. Bioinformatics−led design of single−chain antibody molecules targeting DNA sequences for retinoblastoma. *Int J Ophthalmol* 2011;4(1):8−13

4 Bautch VL, Ambler CA. Assembly and patterning of vertebrate blood vessels. *Trends Cardiovasc Med* 2004;14 (4):138−143

5 Ferrara N. Vascular endothelial growth factor: basic science and clinical progress. *Endocr Rev* 2004;25(4):581−611

6 Jain RK. Molecular regulation of vessel maturation. *Nat Med* 2003;9 (6): 685−693

7 Hicklin DJ, Ellis LM. Role of the vascular endothelial growth factor pathway in tumor growth and angiogenesis. *J Clin Oncol* 2005;23 (5): 1011−1027

8 Naumov GN, Folkman J, Straume O, Akslen LA. Tumor−vascular interactions and tumor dormancy. *Apmis* 2008; 116(7−8):569−585

9 Almog N, Ma L, Raychowdhury R, Schwager C, Erber R, Short S, Hlatky L, Vajkoczy P, Huber PE, Folkman J, Abdollahi A. Transcriptional switch of dormant tumors to fast−growing angiogenic phenotype. *Cancer Res* 2009; 69(3):836−844

10 Holmgren L, O'Reilly MS, Folkman J. Dormancy of micrometastases: balanced proliferation and apoptosis in the presence of angiogenesis suppression. *Nat Med* 1995;1(2):149−153

11 Nussenbaum F, Herman IM. Tumor angiogenesis: insights and innovations. *J Oncol* 2010;2010:132641

12 Ferrara N, Gerber HP, LeCouter J. The biology of VEGF and its receptors. *Nat Med* 2003;9(6):669−676

13 Hanahan D, Folkman J. Patterns and emerging mechanisms of the angiogenic switch during tumorigenesis. *Cell* 1996;86(3):353−364

14 Sledge GW Jr. Vascular endothelial growth factor in breast cancer: biologic and therapeutic aspects. *Semin Oncol* 2002;29(3):104−110

15 Lyons JM 3rd, Schwimer JE, Anthony CT, Thomson JL, Cundiff JD, Casey DT, Maccini C, Kucera P, Wang YZ, Boudreaux JP, Woltering EA. The role of VEGF pathways in human physiologic and pathologic angiogenesis. *J Surg Res* 2010;159(1):517−527

16 Ferrara N. Vascular endothelial growth factor. *Arterioscler Thromb Vasc Biol* 2009;29(6):789−791

17 Gimbrone MA Jr, Leapman SB, Cotran RS, Folkman J. Tumor angiogenesis: iris neovascularization at a distance from experimental intraocular tumors. *J Natl Cancer Inst* 1973;50(1):219−228

18 Rafii S, Lyden D, Benezra R, Hattori K, Heissig B. Vascular and haematopoietic stem cells: novel targets for anti−angiogenesis therapy? *Nat Rev Cancer* 2002;2(11):826−835

19 Kaplan RN, Riba RD, Zacharoulis S, Bramley AH, Vincent L, Costa C, MacDonald DD, Jin DK, Shido K, Kerns SA, Zhu Z, Hicklin D, Wu Y, Port JL, Altorki N, Port ER, Ruggero D, Shmelkov SV, Jensen KK, Rafii S, Lyden D. VEGFR1-positive haematopoietic bone marrow progenitors initiate the pre-metastatic niche. *Nature* 2005;438(7069):820-827

20 Wacheck V, Zangemeister-Wittke U. Antisense molecules for targeted cancer therapy. *Crit Rev Oncol Hematol* 2006;59(1):65-73

21 Tai, W, Qin B, Cheng K. Inhibition of breast cancer cell growth and invasiveness by dual silencing of HER-2 and VEGF. *Mol Pharm* 2010;7 (2):543-556

22 Crawford Y, Ferrara N. VEGF inhibition: insights from preclinical and clinical studies. *Cell Tissue Res* 2009;335(1):261-269

23 Reck M, Crino L. Advances in anti-VEGF and anti-EGFR therapy for advanced non-small cell lung cancer. *Lung Cancer* 2009;63(1):1-9

24 Kukowska-Latallo JF, Bielinska AU, Johnson J, Spindler R, Tomalia DA, Baker JR Jr. Efficient transfer of genetic material into mammalian cells using Starburst polyamidoamine dendrimers. *Proc Natl Acad Sci USA* 1996;93(10):4897-4902

25 Maiti PK, Cagin T, Wang GF and Goddard III WA. Structure of PAMAM dendrimers: Generations 1 through 11. *Macromolecules* 2004;37: 6236-6254

26 Bielinska A, Kukowska-Latallo JF, Johnson J, Tomalia DA, Baker JR Jr. Regulation of in vitro gene expression using antisense oligonucleotides or antisense expression plasmids transfected using starburst PAMAM dendrimers. *Nucleic Acids Res* 1996;24(11):2176-2182

27 Kubasiak LA, Tomalia DA. Cationic dendrimers as gene transfection vectors: dendri-poly (amidoamines) and dendri-poly (propylenimines);

CRC Press: Boca Raton, 2004;Chapter 9:133-157

28 Braun CS, Vetro JA, Tomalia DA, Koe GS, Koe JG, Middaugh CR. Structure/function relationships of polyamidoamine/DNA dendrimers as gene delivery vehicles. *J Pharm Sci* 2005;94(2):423-436

29 Abdelhady HG, Allen S, Davies MC, Roberts CJ, Tendler SJ, Williams PM. Direct real-time molecular scale visualisation of the degradation of condensed DNA complexes exposed to DNase I. *Nucleic Acids Res* 2003; 31(14):4001-4005

30 Shakhbazau A, Isayenka I, Kartel N, Goncharova N, Seviaryn I, Kosmacheva S, Potapnev M, Shcharbin D, Bryszewska M. Transfection efficiencies of PAMAM dendrimers correlate inversely with their hydrophobicity. *Int J Pharm* 2010;383(1-2):228-235

31 Morgan DM, Larvin VL, Pearson JD. Biochemical characterisation of polycation-induced cytotoxicity to human vascular endothelial cells. *J Cell Sci* 1989;94(Pt 3):553-559

32 Rejman J, Bragonzi A, Conese M. Role of clathrin- and caveolae-mediated endocytosis in gene transfer mediated by lipo- and polyplexes. *Mol Ther* 2005;12(3):468-474

33 Gu SZ, Zhao XH, Zhang LX, Li L, Wang ZY, Meng M, An GL: Anti-angiogenesis effect of generation 4 polyamidoamine/vascular endothelial growth factor antisense oligodeoxynucleotide on breast cancer *in vitro. J Zhejiang Univ Sci B* 2009;10(3):159-167

34 Jia RB, Zhang P, Zhou YX, Song X, Liu HY, Wang LZ, Luo M, Lu J, Ge SF, Fan XQ. VEGF-targeted RNA interference suppresses angiogenesis and tumor growth of retinoblastoma. *Ophthalmic Res* 2007;39 (2):108-115